INL/JOU-23-73120-Revision-1

Evaluating Direct Vessel Injection Accident-Event Progression of AP1000 and Key Figures of Merit to Support the Design and Development of Water-Cooled Small Modular Reactors

Palash Kumar Bhowmik

Changing the World's Energy Future

Idaho National Laboratory

INL is a U.S. Department of Energy National Laboratory operated by Battelle Energy Alliance, LLC

INL/JOU-23-73120-Revision-1

Evaluating Direct Vessel Injection Accident-Event Progression of AP1000 and Key Figures of Merit to Support the Design and Development of Water-Cooled Small Modular Reactors

Palash Kumar Bhowmik

February 2024

Idaho National Laboratory
Idaho Falls, Idaho 83415

http://www.inl.gov

Prepared for the
U.S. Department of Energy
Under DOE Idaho Operations Office
Contract DE-AC07-05ID14517

Evaluating Direct Vessel Injection Accident-Event Progression of AP1000 and Key Figures of Merit to Support the Design and Development of Water-Cooled Small Modular Reactors

Hossam H. Abdellatif[a], Palash. K. Bhowmik[b,*], David Arcilesi[a], Piyush Sabharwall[b]

[a]*University of Idaho, 1776 Science Center Dr., Idaho Falls, ID 83402, USA*
[b]*Idaho National Laboratory, 2525 Fremont Ave., Idaho Falls, ID 83415-2209, USA*

habdellatif@uidaho.edu; PalashKumar.Bhowmik@inl.gov; darcilesi@uidaho.edu; Piyush.Sabharwall@inl.gov

Abstract

The passive safety systems (PSSs) within water-cooled reactors are meticulously engineered to function autonomously, requiring no external power source or manual intervention. They depend exclusively on inherent natural forces and the fundamental principles of reactor physics, such as gravity, natural convection, and phase changes, to manage, alleviate, and avert the release of radioactive materials into the environment during accident scenarios like a loss-of-coolant accident (LOCA). PSSs are already integrated into such operating commercial reactors as the Advanced Pressurized Reactor-1000 MWe (AP1000) and the Water-Water Energetic Reactor-1200 MWe (WWER-1200) are adopted in most of the upcoming small modular reactor (SMR) designs. Examples of water-cooled SMR PSSs are the passive emergency core-cooling system (ECCS), passive containment cooling system (PCCS), and passive decay-heat removal system, the designs of which vary based on reactor system-design requirements. However, understanding the accident-event progression and phases of a LOCA is pivotal for adopting a specific PSS for a new SMR design. This study covers the accident-event progression for direct vessel injection (DVI) small-break loss-of-coolant accident (SB-LOCA), associated physics phenomena, knowledge gaps, and important figures of merit (FOMs) that may need to be evaluated and assessed to validate thermal-hydraulics models with an available experimental dataset to support new SMR design and development.

Keywords: AP1000; small-break loss-of-coolant accident; small modular reactor; accident-event progression; passive safety systems; loss-of-coolant accident; accident management

Contents

Nomenclature

ACC	accumulator	LOCA	loss-of-coolant-accident
ACME	advanced core-cooling mechanism experiment	MARS	multi-dimensional analysis of reactor safety code
ACP100	Advanced Chinese Pressurized Reactor-100 MWe	MCCL	minimum collapsed core level
ADS	automatic depressurization system	MIDAC	Module In-vessel Degradation Severe Accident Analysis Code
AP1000	Advanced Pressurized Reactor-1000 MWe	MHAS	multi-dimensional hydrogen analysis system
AP600	Advanced Pressurized Reactor-600 MWe	NC	natural circulation
ARDP	Advanced Reactor Demonstration Project	NPP	nuclear power plant
ARSAC	Advanced Reactor System Analysis Code	PCCS	passive containment cooling system
ATLAS	advanced thermal-hydraulic test loop for accident simulation	PIRT	phenomena identification and ranking table
BEPU	best-estimate plus uncertainty	PRHR	passive residual heat removal
CCFL	counter-current flow limitation	PRHRHXS	passive residual heat removal heat-exchanger system
CFD	computational fluid dynamics	PSS	passive safety system
CI	containment isolation	PSV	pressurizer safety valve
CMT	core makeup tank	PTS	pressurized thermal shock
CRH	control room habitability	PWR	pressurized water reactor
CV	control valve	PXS	passive core-cooling system
DBA	design-basis accident	RCP	reactor coolant pump
DEDVI	double-ended direct vessel injection	RCS	reactor coolant system
DEGB	double-ended guillotine break	SB-LOCA	small-break loss-of-coolant accident
DOE	U.S. Department of Energy	SG	steam generator
DVI	direct vessel injection	SI	safety injection
ECCS	emergency core-cooling system	SIT	safety injection tank
FOM	figure of merit	SMART	system-integrated modular advanced reactor
INL	Idaho National Laboratory	SMR	small modular reactor
IRWST	in-containment refueling water storage tank	SMR-160	small modular reactor-160 MWe
ITL	integral test loop	UDC	upper downcomer

Symbols

: Density (kg/m^3)
: Pressure (MPa)
: Speed of sound (m/s)

1. Introduction

An innovative design aspect shared by both the Advanced Pressurized Reactor-600 MWe (AP600) and the Advanced Pressurized Reactor-1000 MWe (AP1000), which distinguishes them from conventional pressurized water reactors (PWRs), is the incorporation of passive safety features that are aimed at preventing and mitigating the risk of core uncovery in the event of small-break loss-of-coolant accidents (SB-LOCAs) [1][10]. The performance and behavior of the automatic depressurization system (ADS) during a SB-LOCA were studied. This investigation aimed to simulate accident scenarios specific to the AP1000 using the Module In-vessel Degradation Severe Accident Analysis Code (MIDAC) [2]. It is observed that as more ADS valves are opened, the reactor coolant system (RCS) depressurizes more rapidly. This leads to earlier activation of core makeup tanks (CMTs) and accumulators (ACCs), and a more pronounced impact from gravity-driven water injection. However, solely opening ADS1-3 cannot prevent core degradation in scenarios of the first type of accident. The actuation of ADS1-3 significantly influences the injection timing of ACCs and CMTs.

The thermal-hydraulic characteristics of the CMT were examined through various SB-LOCA tests carried out on the advanced core-cooling mechanism experiment (ACME) integral effect test facility [3]. These tests encompassed different break sizes, including 2.5 cm, 5 cm, and 20 cm breaks, as well as a double-ended direct vessel injection (DEDVI) line break scenario. The study demonstrated that the CMT response to a SB-LOCA was categorized into four distinct phases: circulation, drain transition, injection inhibition, and final drainage. The break condition has significant impacts on the CMT operating characteristics in each phase. In addition, the injection of nitrogen gas into the ACC continued to influence the drainage behavior of CMT. An 8.5-inch DEDVI nozzle was replicated using the advanced thermal-hydraulic test loop for accident simulation (ATLAS) facility [4]. A parallel test involving an equivalent rupture size was conducted at the cold-leg to facilitate a comprehensive comparison using the multi-dimensional analysis of reactor safety (MARS-KS) code [5]. The investigation revealed that partial core uncovery is evident in both scenarios. Notably, across all four cases, in addition to encompassing the experimental data, the direct vessel injection (DVI) line break case consistently proves to be more restrictive than the corresponding cold-leg break case in terms of limiting outcomes. The MARS-KS code's predictive accuracy was deemed acceptable; however, it did not adequately reproduce the behavior of water levels in both the core and downcomer regions.

A recent study used the best-estimate plus uncertainty (BEPU) method to carry out a comprehensive analysis of DEDVI line rupture in the Advanced Chinese Pressurized Reactor-100 MWe (ACP100) small modular reactor (SMR) system using Advanced Reactor System Analysis Code (ARSAC) [6]. The results revealed that optimizing coolant performance in the minimum collapsed core level (MCCL) can enhance the safety margins. This involves tuning parameters like loss coefficients and pipe diameters. Improving constitutive models, including the critical flow and interfacial friction models in the ARSAC code, will refine uncertainty analysis, providing a more accurate depiction of potential outcomes and uncertainties. An experimental study was conducted to examine the thermal-hydraulic characteristics of SB-LOCA experiments within an integral test loop (ITL) associated with a system-integrated modular advanced reactor (SMART) [7]. This investigation focused particularly on the occurrences involving the pressurizer safety valve (PSV) line and safety injection (SI) line breaks. It was observed that four consecutive phases were identified in the sequence: initial blowdown to the upper downcomer (UDC) saturation, followed by a pressure plateau during forced circulation, subsequent boil-off following the reactor coolant pump (RCP) trip, and eventual restoration of core levels following injection of safety injection tank (SIT) coolant or through prolonged cooling measures.

A transient assessment model carried out for AP1000 SB-LOCA analysis during the transition from CMT injection to in-containment refueling water storage tank (IRWST) injection. The model effectively replicates key processes including ADS-4 activation, CMT injection, IRWST injection, monitoring of reactor core mixture levels, and consideration of entrainment phenomena in the upper plenum toward the hot-legs [8]. The results showed that the passive emergency core-cooling system (ECCS) effectively ensures sufficient cooling to prevent any instance of reactor core uncovering throughout the entire duration of the transient event. The sensitivity analysis conducted on ADS-4 flow resistance indicates that increased resistance results in a postponement of IRWST injection. However, even with this delay, the

injection of IRWST continues to deliver a satisfactory flow rate, effectively covering the active core region.

When designing a reactor system, it is always important to understand the reactor system accident-event progression and associated physical phenomena [9]. Loss-of-coolant accidents (LOCAs) for water-cooled SMRs entail very specific accident-event progressions, including the initiation and activation of passive safety systems (PSSs) [10]. A LOCA is a hypothetical accident scenario in which the coolant in a nuclear reactor becomes unavailable due to a breach in the primary coolant piping system or a failure in the reactor's cooling mechanisms. This can cause a loss of cooling capability and a rapid rise in fuel temperature, possibly leading to fuel damage and the potential release of radioactive materials [11]. Reactor PSSs are designed to mitigate the consequences of LOCAs by using the inherent physics of the reactor, such as gravity, natural convection (NC), and phase changes, to cool the reactor and prevent the release of radioactive materials. Examples of PSSs in water-cooled SMRs include the passive ECCS, passive containment cooling system (PCCS) [11],[12],[13], and passive decay-heat removal system [10]. To effectively implement a PSS, it is important to thoroughly identify the accident-event progression and associated phenomena. Such phenomena can include the behavior of coolant and steam during a LOCA, the behavior of fuel rods as they heat and potentially melt, and the behavior of gases and aerosols as they are released from the reactor [11],[12], [13], [14],[15].

Additionally, evaluating PSS performance requires using figures of merit (FOMs), such as peak cladding temperature, time to core uncovery, and maximum pressure in the containment vessel. These FOMs can be used to assess the effectiveness of different PSSs and compare the performance of different SMR designs. Thermal-hydraulics models can simulate reactor behavior during a LOCA and evaluate PSS performance. However, these models must be validated using supportive test datasets in order to ensure their accuracy and reliability [13],[14],[16]. In short, understanding the accident-event progression and physical phenomena associated with LOCAs is crucial for effectively implementing PSSs in water-cooled SMRs and ensuring the safety of nuclear power plant (NPP) reactors.

Conducting a comprehensive and independent investigation into the reliability of the passive safety features of the AP1000 is crucial, given its robust design. This endeavor is essential to enhance the plant safety measures significantly. Therefore, it is imperative to conduct a detailed assessment of plant response during transient conditions. The primary goal of this research is to deliver readers a comprehensive, up-to-date understanding of the DEDVI line break scenario, its associated thermal-hydraulic phenomena, and the capability of a PSS in managing such transients. This paper strives to establish a critical foundation and conceptual framework that not only reconciles and builds upon prior research, but also serves as a catalyst for new investigations. The overarching objective is to advance the FOM for the secure operation of the AP1000, which, in turn, contributes to the research and development (R&D) progress of SMRs that rely on PSSs. There are several light water-based SMRs, such as the system-integrated modular advanced reactor (SMART), Advanced Pressurized Reactor-300 MWe (AP300), and United Kingdom small modular reactor (UK-SMR) [17],[18],[19]. The AP300 SMR is a one loop PWR with 300 MWe (990 MWth). Utilizing the proven passive containment and core cooling systems, it adopts the same approach of the AP1000 plant while incorporating specific modifications to enhance its performance. It is worth noting that the SMART design adopted similar PSSs as the AP1000 and AP300, such as the passive residual heat removal system (PRHRS) and IRWST. Ensuring the safety of next-generation reactors requires precise evaluation of accident scenarios and a thorough assessment of the reliability of their PSSs. Therefore, an understanding of system behavior following a DEDVI line break will help improve the design and license of next generation SMRs, including the small modular reactor-160 MWe (SMR-160), by relying on PSSs like the AP1000 reactor.

2. Description of the AP1000 PSS

The AP1000 PSSs are designed to mitigate design-basis accidents (DBAs) without the need for operator intervention. These systems rely on passive mechanisms, such as gravity, NC, and the release of compressed gas to carry out their safety functions. Active machinery—such as pumps, fans, diesel generators, and chillers—are not employed, apart from the valves that activate the PSS.

To ensure reliability, the valves are designed to move to their safeguard positions in the event of power loss or the receipt of a safeguard-actuation signal and are powered by multiple dependable Class 1E direct current (DC) power batteries. Unlike with typical NPPs, the AP1000 PSSs do not need a large network of active-safety support systems, such as alternating-current (AC) power; diesel generators; heating, ventilation, and air conditioning (HVAC); and pumped cooling water. Consequently, these active support systems can be simplified or eliminated, and no longer need to be represented by a safety class. The elimination of safety-grade equipment reduces the size of the seismic Category 1 building spaces required to house them. Furthermore, most safety equipment can now be located within the reactor containment, leading to fewer containment penetrations.

The various AP1000 PSSs can be classified as shown in *Fig. 1*, with a PCCS, containment isolation, and main control-room habitability system, as shown in Fig. 2. This study focuses on the passive core-cooling system (PXS), which will be described in greater detail within the context of a small-break loss-of-coolant-accident (SB-LOCA) for the AP1000 [20],[21].

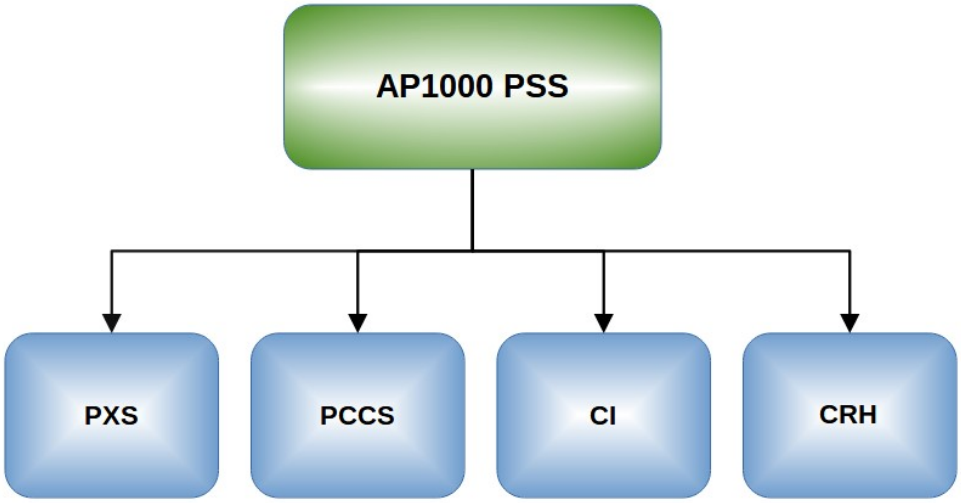

Fig. 1. AP1000 PSS classification.

2.1. Major Functions of the PXS

The two major functions of the PXS are:

1. Safety injection and reactor coolant makeup, which include:
   - CMTs
   - ACCs
   - IRWST
   - Long-term core-cooling recirculation
   - ADSs
2. PRHRS, which includes:

- The PRHR heat-exchanger system (PRHRHXS)
- IRWST.

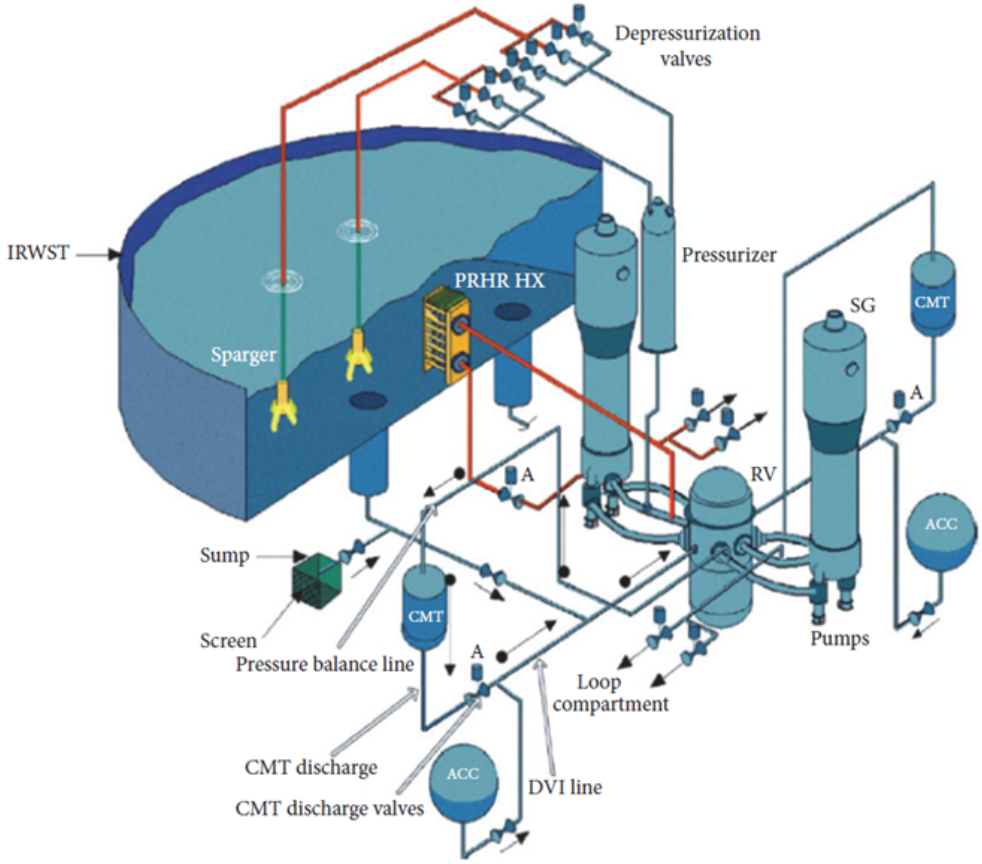

Fig. 2. AP1000 PXS [19-21].

2.2. Core Makeup Tanks

The two CMTs are slightly elevated above the reactor core and are connected to the reactor coolant system (RCS) via a discharge injection line and an inlet pressure-balance line. To keep the CMT pressure equal to that of the primary system, the top of the CMT is connected to the cold-leg. The outlet or bottom part of the CMT is connected to the DVI line via the discharge line, as can be seen in Fig. 2. Additionally, two parallel air-operated valves are present on the CMT discharge line. These valves are normally open and serve to isolate the CMT discharge line from the DVI line [22].

2.3. Passive Residual Heat Removal System

The PRHRHXS operates by using passive processes, such as gravity and NC. It serves as the primary component of the PRHRS and is situated in the IRWST, which acts as a heat sink, as observed in Fig. 3.

The PRHRHXS consists of a C-shaped tube bundle for extracting core decay heat from the RCS if specific postulated accidents cause one or more steam generators (SGs) to cease operation. Cold coolant in the RCS is kept at full pressure in the PRHRS, which is connected to the RCS via a tee from one of the fourth-stage automatic depressurization lines [23],[24],[25].

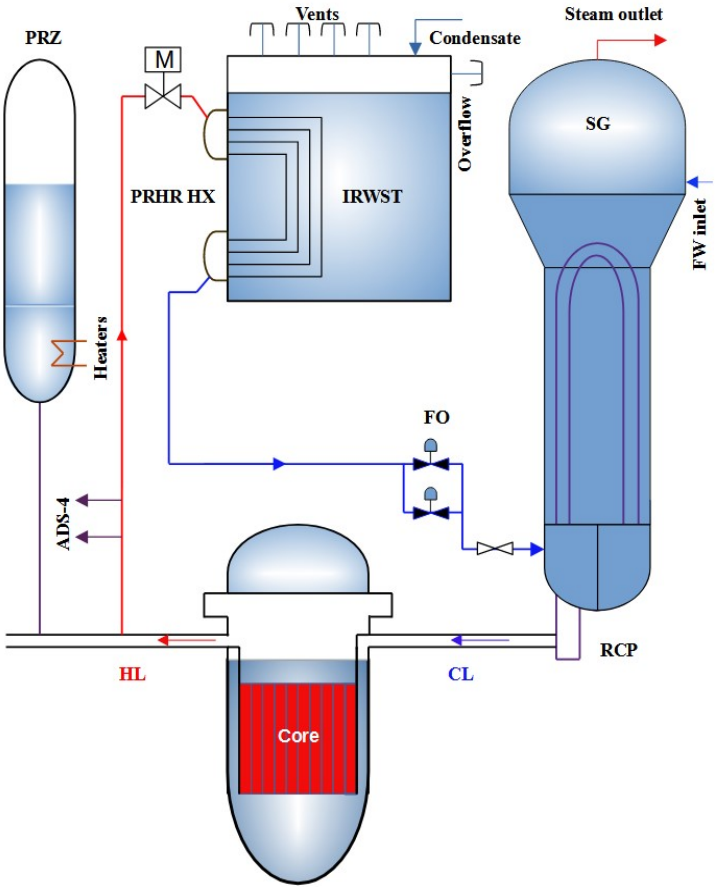

Fig. 3. Schematic of the AP1000 PRHRS.

2.4. Automatic Depressurization System

The ADS consists of four stages, each containing valves that progressively reduce pressure in the primary system. Two sets of valves comprise the first three stages, which are connected to the top of the pressurizer. Activation of these stages is tied to the CMT liquid level. When the CMT liquid level drops to 67.5% of its original volume, the first stage is activated, with the second and third stages after 70 and 120 seconds, respectively. These stages vent steam from the primary system through the ADS-1, -2, and -3 valves, which lead the steam into the sparger line that guides it toward the IRWST. Here, the steam is condensed via direct contact with highly subcooled water.

The fourth-stage of the ADS involves two large valves connected to the ADS lines on each hot-leg. The ADS-4 valves are designed to open when the CMT liquid level drops to 20% of its original value. This mechanism effectively lowers the pressure on the primary side so as to align it with containment conditions. The discharge from the ADS-4 valves is then released directly into the containment building [9].

2.5. Accumulators

ACCs are substantial spherical tanks filled to approximately 75% capacity with cold-borated water. They are pre-pressurized using nitrogen gas. ACC outlet lines are connected to the DVI line with a pair of check valves installed to inhibit injection flow during normal operation. However, when the system pressure falls below both the pressure within the ACCs and the opening or “cracking” pressure of the check valves, these valves open, allowing coolant to be dispatched into the reactor downcomer via the DVI line.

2.6. In-containment Refueling Water Storage Tank

The IRWST is a sizable concrete pool filled with cold-borated water. It serves a dual function, acting as a heat sink for the PRHRHXS and providing a water source for IRWST injection. The IRWST is equipped with two injection lines that connect to the DVI lines of the reactor vessel. Under normal conditions, these flow paths are isolated by two check valves, in series. However, if the primary system pressure drops below the head pressure of the IRWST water, a flow path is established through the DVI. This allows water from the IRWST to be introduced into the reactor vessel downcomer. The volume of water stored in the IRWST is enough to flood the lower containment compartments, effectively raising the water level above the reactor vessel head and to a point just beneath the outlet of the ADS-4 lines [24],[26].

3. Description of the SB-LOCA Scenarios and Accident Phases

In safety assessments conducted for the AP1000, a SB-LOCA was characterized as a reactor coolant pressure-boundary rupture involving a total cross-sectional area of less than 1.0 ft^2. Such occurrences are classified as Condition III events, a categorization that denotes infrequent faults that may arise over the operational lifespan of the plant [27].

3.1. DVI-DEGB SB-LOCA Scenarios

A direct vessel injection double-ended guillotine break (DVI-DEGB) refers to a double-ended rupture of the 8-in. pipe near the DVI nozzle, as indicated in Fig. 4, leading to two distinct sources of coolant discharge. One source (on the vessel side) results in reactor depressurization, while the other causes the ACC and CMT to release coolant into the containment. As a result, only one of the two passive safety injection systems is involved in responding to the break sequences.

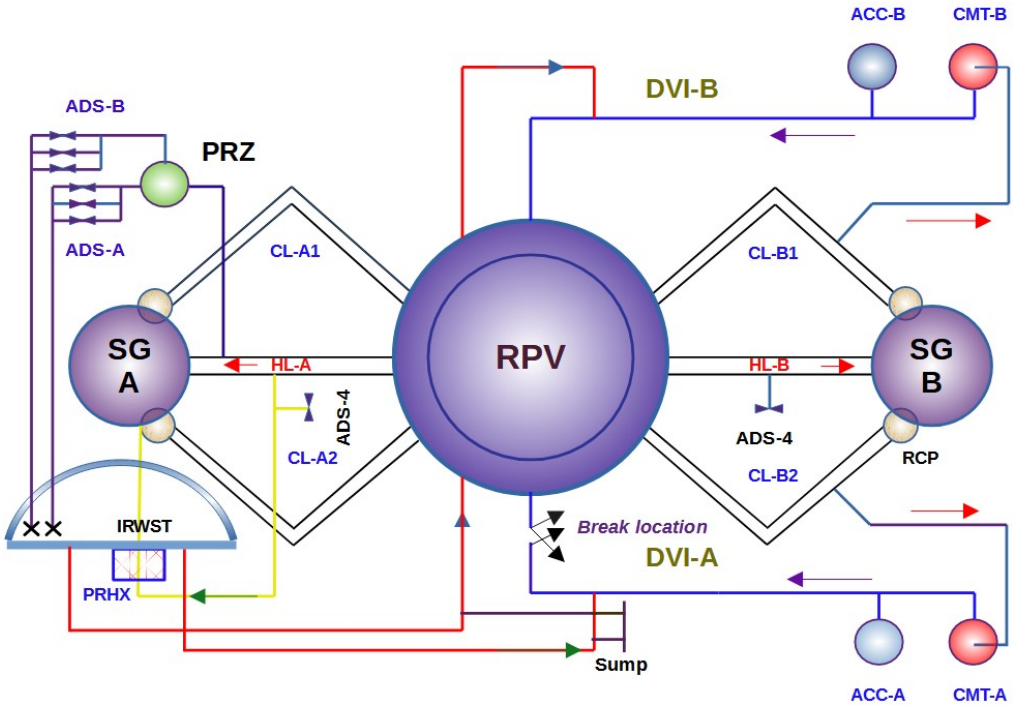

Fig. 4. RCS and passive safety injection systems in the event of a DVI line break.

During a postulated DVI-DEGB SB-LOCA, the AP1000 NPP will experience several crucial events, including depressurization of the primary coolant system, inventory depletion, inventory replacement using the PXS, and rejection of decay-heat to the atmosphere over the long-term. Four distinct periods have been identified in describing the AP1000 SB-LOCA event: (1) break depressurization, (2) depressurization via ADS discharge to the IRWST, (3) depressurization via ADS discharge to the containment, and (4) long-term cooling. Table 1 shows the detailed sequence of the AP1000 DEDVI event for Westinghouse code (NOTRUMP) and TRACE code[24],[28],[29].

Table 1. DEDVI break time sequence event (NOTRUMP vs. TRACE) [29].

Event	NOTRUMP code (s)	TRACE code (s)
Break Initiation	0.0	0.0
Reactor trip	13.1	20
Safeguard signal (S)	18.6	26
Turbine trip	19.1	26
RCP trip	24.6	32
PRHR actuation	26	34.1
CMT injection starts	29	44.1
ADS-1 starts	182.5	176
ADS-2 starts	252.5	224
Intact ACC starts	254	234.3
ADS-3 starts	372.5	344
ADS-4 starts	492.5	472
Intact ACC empties	600	648
IRWST injection starts	1470	1040.9

A comparison between the two mentioned codes can be seen in Fig. 5. The sequence of events is ordered from 1–15 from the break opening to the IRWST injection, respectively. It should be noted that the TRACE code well predicted the different events with little discrepancies as compared with the NOTRUMP code. The differences between the two codes may refer to the influence of the conservative models and hypotheses integrated into the SB-LOCA licensing analysis that was carried out with the NOTRUMP code.

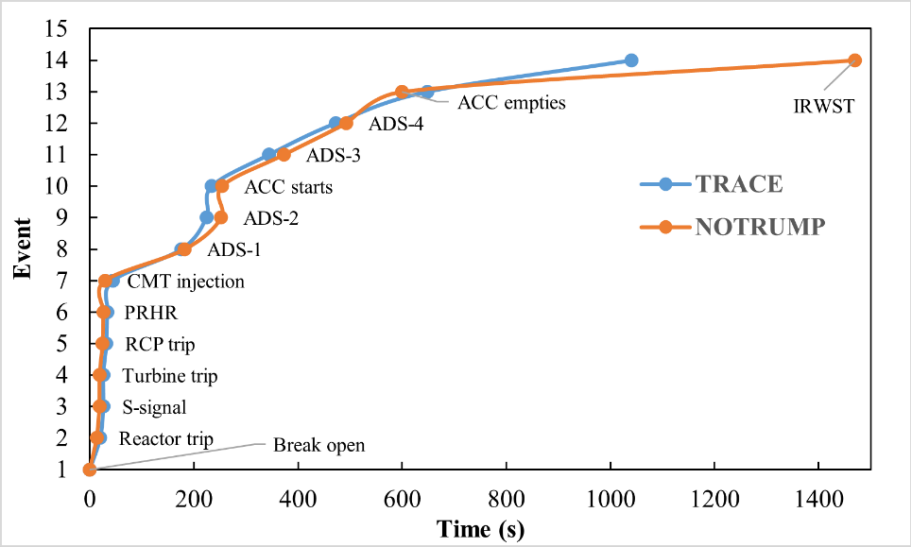

Fig. 5. DEDVI chronology comparison between the NOTRUMP and TRACE codes.

3.2. DVI-DEGB SB-LOCA Phases

In the context of a DVI-SB-LOCA-DEGB, the following four distinct phases in the AP1000 reactor can be distinguished:

I. Blowdown Phase

During the blowdown phase, the reactor experiences a decrease in initial pressure, thereby triggering the reactor trip and an "S" signal. It is important to observe that opening the CMT and PRHRS valves creates three new NC paths that help cool the core, thus causing the RCS pressure to drop below that of the SG pressure.

II. Natural Circulation Phase

The NC phase is characterized by the cooling of the primary system through various NC paths, such as the CMTs (*blue path*) and PRHRS (*yellow path*), as well as via the break and the SGs, as observed previously in Fig. 5. This phase ends with the activation of ADS-1. Unlike in conventional PWRs, SGs in the AP1000 play a lesser role during SB-LOCAs due to early activation of the PRHRS and use of the IRWST as the primary heat sink. During the recirculation mode of the CMTs, the water in the upper portion of the tanks is gradually replaced with vapor. This process continues until the level in the CMT decreases to the point that the ADS is triggered.

III. ADS Blowdown Phase

Once the level in the CMTs reaches approximately 67.5% of its initial value, the automatic opening of the ADS-1 valves initiates the blowdown phase of the ADS. Following a brief delay, ADS stage-2 and stage-3 are activated, representing depressurization to the IRWST stage. Subsequently, when the CMTs reach around 20% capacity, the ADS-4 valves are triggered, causing depressurization to the containment. As a result of the pressure reduction caused by the ADS valves and the break, the setpoint for actuating the ACC charging pumps is achieved at 49 bar. This enables the borated water in the ACC to drain into the RCS and prevent partial or complete flow from the CMTs due to the larger ACC flow.

IV. Long-term Core-Cooling

The long-term cooling phase begins after activation of the IRWST and continues indefinitely. The IRWST will be depleted within a few days, at which point, water from the sump will be circulated continuously. The DVI lines convey water from the IRWST to the vessel downcomer for heating in the core, causing evaporation and creating a two-phase liquid level in the core. Steam produced in the core is then released to the containment through ADS-4.

During the long-term cooling phase, the PCCS plays a crucial role. Any steam released into the containment via the break or ADS-4 condenses on the inner surface of the steel containment shell and drains downward to the IRWST or sump via gutters. Heat transfer on the external surface of the steel containment shell takes place through water evaporation and natural air circulation driven by buoyancy. This process continues until the water supply to the PCCS is depleted. Afterward, the buoyancy-induced airflow alone is adequate to remove the decay-heat released into the containment.

The SB-LOCA chronology of the AP1000 PSS is shown in Fig. 6, which summarizes the different phases discussed above.

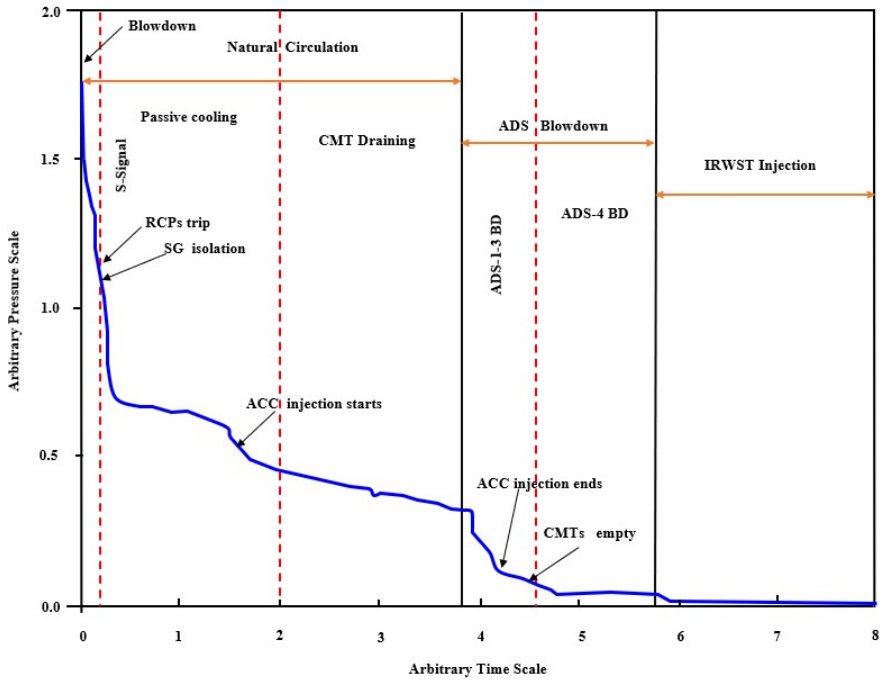

Fig. 6. AP1000 SB-LOCA pressure transient.

4. Knowledge Gaps and Findings/Discussion

In Chapter 15 of the AP1000-design control document [30], the ability of the plant to handle a medium-sized break with only half its total passive safety injection capability is evaluated by analyzing a specific sequence. The DVI line is 6.8 in. in diameter, but the effective break size is limited by a 4-in. diameter flow restrictor on the vessel side, thus restricting the maximum flow that can be depleted through the break. Consequently, the event is classified within the SB-LOCA category. Notably, in this type of sequence, one CMT, one ACC, and one IRWST injection line become unavailable due to the location of the break, thereby setting it apart from other SB-LOCAs (e.g., hot- and cold-leg SB-LOCAs). The DVI-DEGB break sequence is the one that most contributes to the core-damage frequency in the AP1000, accounting for 39.4% of the total core-damage frequency, as shown in Fig. 7 [30],[31].

The design control document includes two separate analyses of DVI-DEGB line breaks. These analyses were conducted at different containment pressures: 20 psi (1.38 bar) and 14.7 psi (1.0135 bar); and utilized the NOTRUMP code in tandem with the WGOTHIC containment model [32].

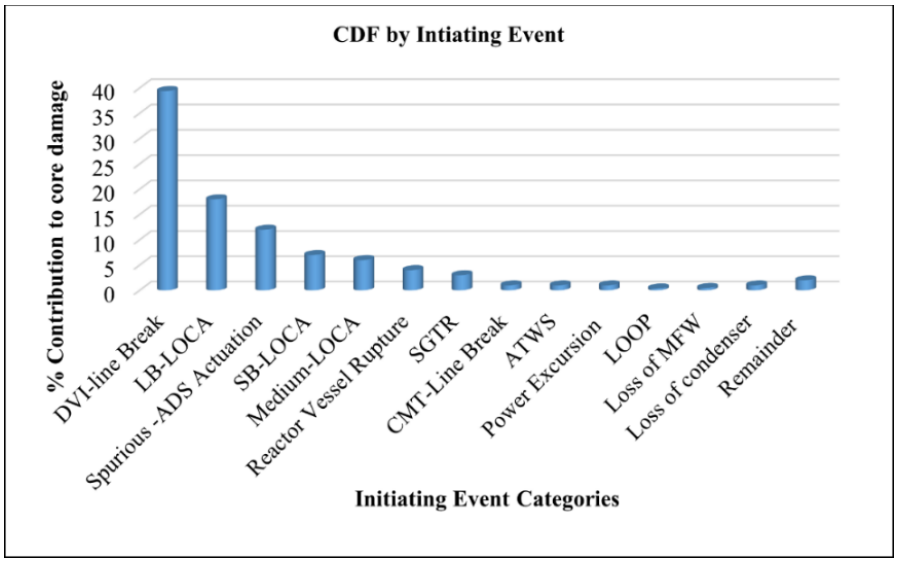

Fig. 7. Contribution to core-damage frequency of the initiating events.

4.1. RCS Pressure

Assuming an instantaneous opening at time $t = 0$ s, the ACC connected to the broken loop starts discharging through the DVI line into the containment. The subcooled discharge emerging from the downcomer nozzle rapidly depressurizes the RCS, as illustrated in Fig. 8. When a reactor trip signal is detected, an "S" signal is generated, thereby initiating a predetermined sequence of actions.

After a specific delay, the isolation valves on the CMT and PRHRS delivery lines are commanded to open. The "S" signal also instructs the main feedwater isolation valves to close following a 2-second delay, and the RCPs are shut down after a delay of 6 seconds.

Opening of the CMT isolation valves allows the broken loop CMT to discharge directly into the containment. This establishes a minor circulating flow through the CMT of the intact loop.

After the break initiation, the RCS experiences a rapid drop in pressure, as both mass and energy release through the break. Simultaneously, the flow on the vessel side of the rupture significantly decreases due to the formation of vapor near the break, which increases the resistance to fluid flow. As the coolant undergoes a phase change, transitioning to vapor in the hotter regions of the RCS, the primary depressurization rate initially slows down rapidly and eventually stalls. The break dominant depressurization characterizes the first period until the ADS1-3 starts around 182.5 seconds. The second stage can be characterized by the RCS depressurization due to the ADS1-3 discharge to the IRWST.

By comparing the pressure trend during a DEDVI break for both containment cases, it can be observed that the RCS pressure trend for both cases of containment pressure is quite similar during the entire transient. Concerning the containment pressurization, the ADS-4 starts to discharge into the containment around 500 seconds leading to an increase in containment pressure, as shown in Fig. 8. Once the CMT resumes after emptying the intact ACC, the containment pressure tends to decrease in an oscillatory manner linked to ADS-4. During the long-term cooling phase, the containment pressure reduces linearly to reach a value close to 23 psia and 18 psia for 20 and 14.7 psia containment pressure cases, respectively.

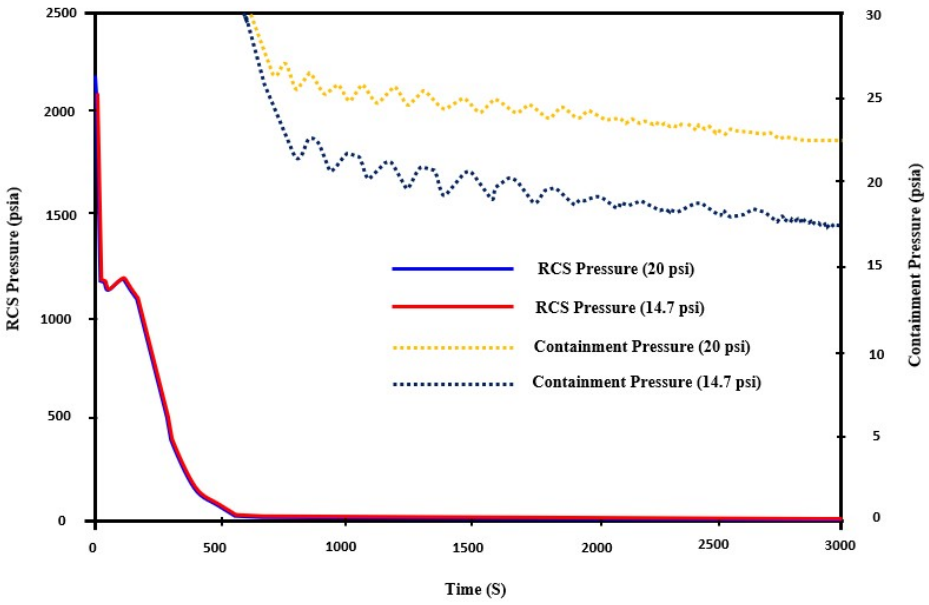

Fig. 8. DVI-DEGB-RCS pressure [23].

4.2. Mixture Level

As the pressure drops, the fluid in the RCS reaches saturation, forming a mixture level in the upper plenum. This mixture level drops down to the hot-leg elevation, as observed in Fig. 9. This initiates drainage of the upper sections of the RCS, creating a mixture level in the downcomer that descends below the elevation of the break. This leads to a two-phase discharge and vapor flow from the downcomer side of the break.

Simultaneously, the level in the CMT linked to the broken loop diminishes, ultimately hitting the setpoint for the first stage of ADS-1. Once the signal delay has passed, the ADS-1 valves are triggered to open. Consequently, steam released from the top of the pressurizer leads to an increased rate of depressurization in the RCS. This depressurization rate is further accelerated by the venting of steam from the downcomer to the containment, which happens when the mixture level in the downcomer drops below the level of the DVI nozzle.

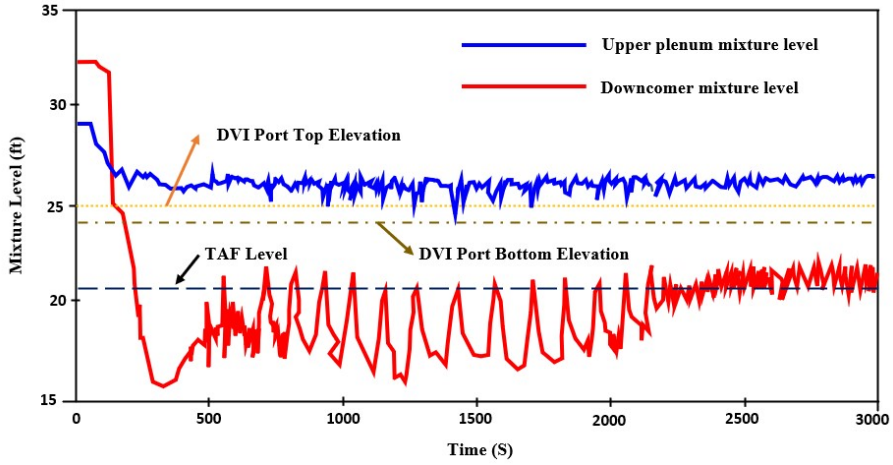

Fig. 9. Mixture level in the core upper plenum and downcomer [23].

ADS-2 is activated following an appropriate time delay after the first stage. Subsequently, the ACC in the intact loop begins to inject into the downcomer, gradually raising the mixture level in the downcomer, as shown in Fig. 10. This consequently raises the mixture level in the upper plenum. ADS-3 is triggered after a time delay of 120 seconds between the activation of ADS-2 and ADS-3. Even though the CMT level in the broken loop reaches the ADS-4 setpoint, the stage 4 valves do not open until the minimum time delay between the activation of ADS-3 and ADS-4 has passed. As a result, a two-phase discharge occurs through three of the four Stage 4 paths. The CMT and ACC in the broken loop deplete rapidly.

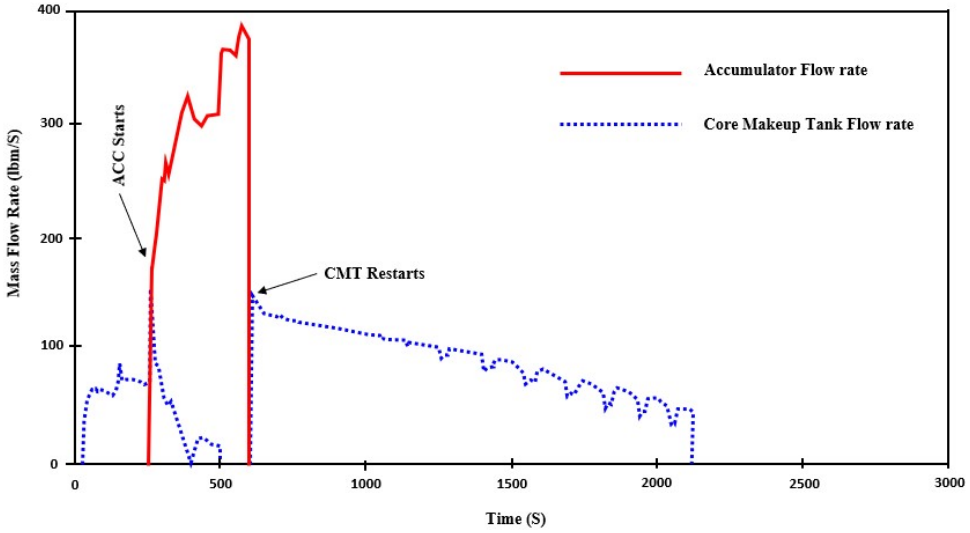

Fig. 10. Intact loop ACC and CMT flow rate [23].

The gradual decrease in fluid level at the top of the intact loop CMT is due to the initiation of injection from the tank, as shown in Fig. 10. The intact loop ACC has been emptied, allowing for continuous injection of the CMT due to the reduced pressure in the injection line.

The downcomer mixture level slowly rises during the ACC injection. Fig. 11 illustrates the RCS mass inventory as compared with a 2-in. cold-leg break. Since the intact loop CMT injection is only available for a certain period, the downcomer level once again decreases, causing an increase in the RCS inventory depletion rate—due to core boil-off—until sufficient CMT/IRWST injection flow can be introduced. However, the level in the upper plenum is maintained at near the hot-leg elevation throughout the rest of the transient. When the pressure in the broken DVI line falls below that in the IRWST, water from the tank spills into the containment.

As the RCS pressure gradually drops, injection from the intact loop CMT continues at a stable but decreasing rate. The pressure continues to decrease until it falls below that of the IRWST; at which point, injection commences. Due to the reduced initial inventory recovery from the ACCs and only a single intact injection path available for the DEDVI line break, the minimum inventory is reached near the start of the IRWST injection flow. However, once an injection flow exceeding the sum of the break and ADS flows is achieved, the RCS inventory slowly increases. Fig. 11 clearly shows that the mass inventory depletion was faster for the DVI break than for the 2-in. break, indicating that break size significantly impacts the depletion rate.

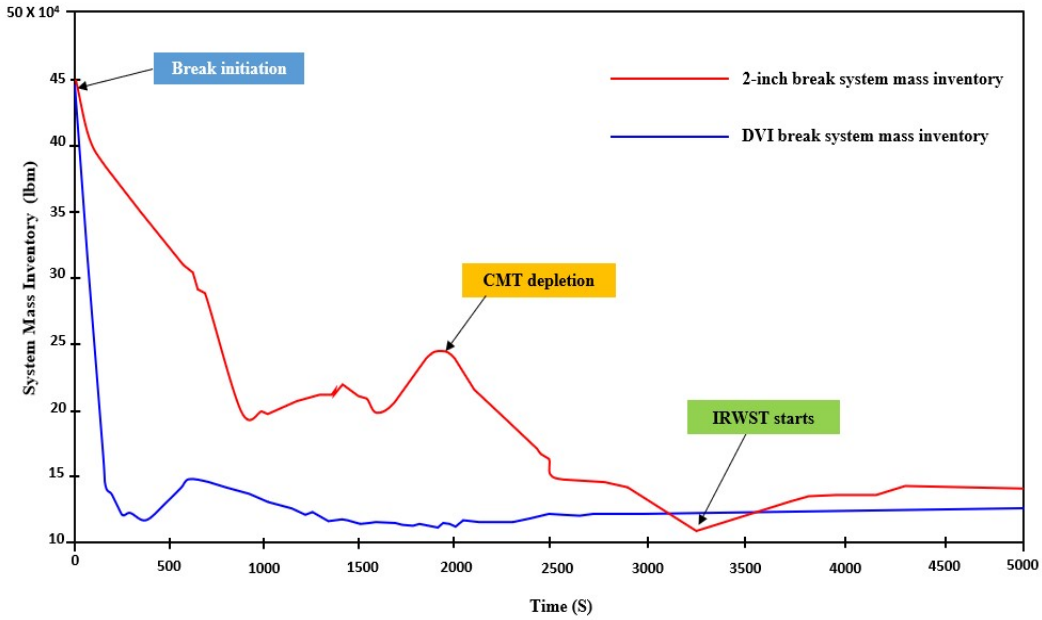

Fig. 11. RCS mass inventory during a DVI-DEGB and a 2-in. break [23].

Due to the sufficient mass inventory of the RCS, the SB-LOCA in the DEDVI scenario does not result in the core being uncovered, thus allowing for extended cooling until the system is recirculated in the containment. Proper flow is maintained through the core, preventing any increase in fuel-rod temperature or the accumulation of boric acid. Moreover, the wall-to-wall flooding case examined via the window-mode technique illustrates effective core-cooling, even at the minimum containment water level. These outcomes validate the efficacy of AP1000 PSS in facilitating extended cooling during constrained LOCA events.

4.3. Fuel-Rod Surface Temperature

The acceptance criteria for LOCAs, outlined in 10 CFR 50.46 [33], are shown in Table 2.

Table 2. Emergency core-cooling system acceptance criteria.

Parameter	Acceptance design limit
Maximum fuel-element cladding temperature	less than 2200°F
Maximum total cladding oxidation	less than 0.17 times the cladding thickness prior to oxidation
Total hydrogen generation	<1% of the total amount if all zirconium were to react
Coolable geometry under transient conditions	
Long-term core-cooling capability	

In the case of DVI-DEGB, a sufficient core flow is ensured so as to maintain a low cladding temperature and prevent the accumulation of boric acid on the fuel rods, as shown in Fig. 12.

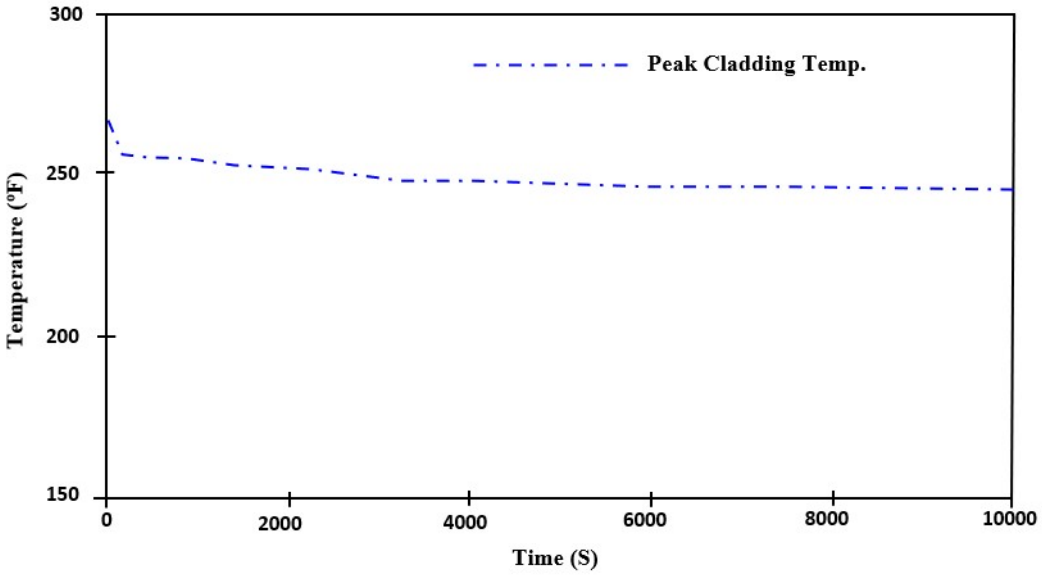

Fig. 12. Peak cladding temperature for DVI-DEGB [23].

4.4. Important Thermal-Hydraulic Phenomena during the DEDVI Accident (SB-LOCA)

The FOMs identified in the phenomena identification and ranking tables (PIRTs) indicate whether the integrity of the reactor safety barriers have been jeopardized. The radiological barriers include:

- Fuel cladding
- RCS pressure boundaries
- Containment pressure boundaries.

Based on the AP600 SB-LOCA PIRTs, which form the basis for the PIRTs used for the AP1000, the ranking criteria are divided into two main phases—the short- and long-term phases—each with its paramount phenomena and parameters, as shown in Fig. 13. On the one hand, the significance of the CMT level and ADS flow rate increases during the later stages of the short-term phase because they play a crucial role in determining the timing of ADS staging and the rate at which the RCS is depressurized. On the other hand, the RCS-to-containment differential pressure takes precedence as the key parameter in the long-term phase by directly influencing the magnitude of the IRWST and sump-injection flow rate [34],[35]. As evident from the AP1000 system unavailability data presented in

Table 3, it can be observed that the highest unavailability values ranging from 10^{-2} to 10^{-3}, indicative of lower reliability are linked to non-safety-related systems or functions. Conversely, the lower unavailability values ranging from 10^{-4} to 10^{-6}, indicating higher reliability, are associated with safety-related systems. Moreover, it is worth noting that most of the PSSs include ACCs, CMTs, PRHRS, and ADSs have a higher reliability as compared with the active components [31].

Table 3. Typical AP1000 system failure probabilities [34].

Failure System/Function	Probability
CMT valve signal	5.7E-07
PRHR valve signal	1.1E-06
PCCS	1.8E-06
Reactor trip by PMS	1.2E-05
ACCs	6.9E-05
IRWST injection	6.9E-05
ADS	9.3E-05
Passive RHR	2.0E-04
CMTs	1.1E-04
RCP trip	5.9E-04
Containment isolation	1.6E-03
Diesel generator	1.0E-02
Condenser	2.4E-02
Main feedwater	2.8E-02
Hydrogen control	1.0E-1

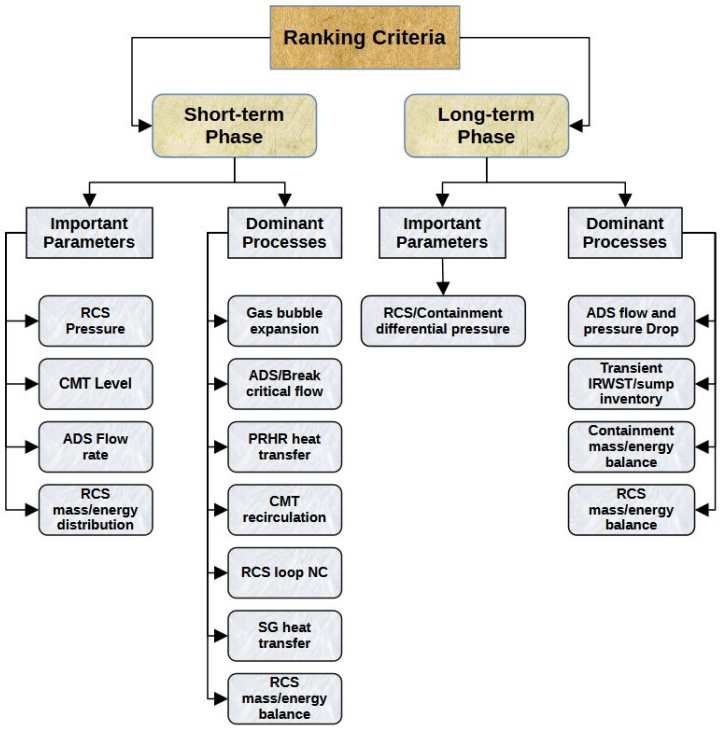

Fig. 13. SB-LOCA ranking criteria for the AP600.

4.4.1. ACC N2 Injection Behavior

Certain phenomena should be considered during the DEDVI transient. In the DEDVI scenario, the ACC injection of nitrogen gas (N_2) significantly affects the CMT injection and delays the start of IRWST drainage, causing a reduction in the minimum core level. The influence of N_2 gas on the DEDVI break transient is notable. Nevertheless, despite the decrease in core inventory, the peak cladding temperature remains unaffected.

In situations involving a small-break in the main pipe prior to activation of ADS-4, N_2 gas is partially released. This mitigates the effects of N_2 gas injection on system responses and core safety during the ADS-4 depressurization phase. However, during a DEDVI event, the ACC N_2 gas is fully discharged into the system following ADS-4 activation. This amplifies the effects of N_2 gas injection, inhibiting CMT drainage and delaying the start of the IRWST injection. When ACC emptying occurs post-ADS-4 activation, the impact of N_2 gas injection must be considered because it lowers the core level.

Despite these effects, the quantity of injected N_2 gas and its heat-absorption capacity are minor compared to the vapor generated within the system and the heat produced by core decay power. For the current passive safety plant design, the pressurization effect of the injected N_2 gas is too small to directly impact system depressurization [36].

4.4.2. Natural Circulation

Fig. 14 depicts the flow regimes anticipated for PWRs with SG U-tubes featuring different coolant-mass inventories. These identified flow regimes may be viewed as indicative scenarios in the event of an SB-LOCA involving gradual depletion of coolant mass in the primary system. Note that the mass-flow rate at the core inlet is dependent on the mass inventory of the primary system. In addition to considering the various flow regimes, attention should be given to the transition zones and the occurrence of a dryout situation, which typically happens when the mass inventory is below approximately 40% of the nominal value. Dryout is caused by a significant decrease in the heat transfer coefficient within the core, as triggered by the void fraction and mass velocities reaching a lower boundary [37].

During single phase NC, the entire primary system is in a single phase, and the pressurizer is losing mass to compensate for the break flow. The SG heat sink is available, and there is a possibility of flow reversal in the U-tubes, resulting in an increase in pressure drops due to a reduced cross-flow area for the overall system under NC.

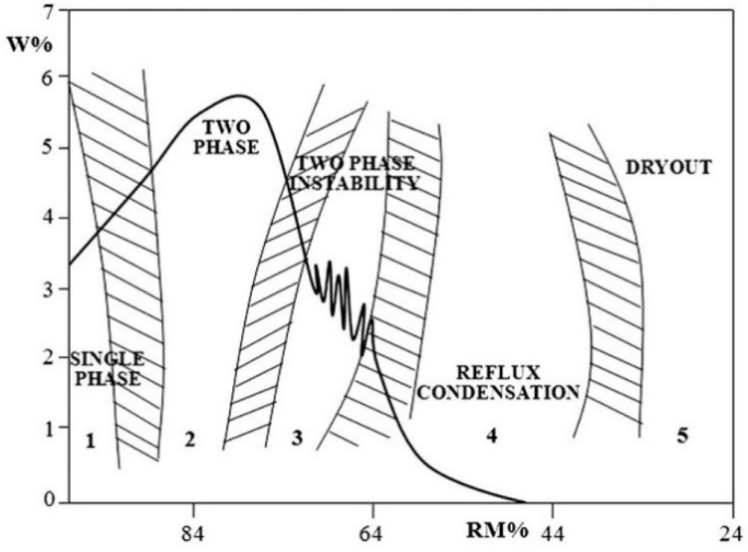

Fig. 14. Natural circulation flow regimes [38],[39].

On the other side, the two-phase NC regime covers the ascending part of the curve, the area of maximum value, and the initial section of the descending segment. This phase initiates with the formation of voids, which is stimulated by simultaneous boil-off in the core and depressurization caused by a break. The upward part of the curve results from a positive balance between the driving head and pressure drops as the coolant-mass inventory diminishes. A state of equilibrium is achieved at the peak region, and further mass reduction leads to a negative balance between the driving head and pressure drops. This may potentially cause a flow reversal in the U-tubes [40],[41].

When the RCS experiences flashing and boiling, it generates enough steam to have it flow into the SGs and collect at the top of the SG U-tubes. At this point, NC stops because the driving force cannot overcome the resistant force in the NC loop. Once the flow stagnates, the mixture levels in both the upward and downward sides of the U-tube SG gradually decrease, causing the NC to transition into the reflux condensation mode [42],[43].

Siphon condensation oscillations are initiated by the counter-current flow limitation (CCFL) at the U-tube entrance, the formation of liquid inside the U-tubes due to condensation or heat removal from the SG, and the liquid level rising until it reaches the top of the relevant U-tubes. The sudden drainage of liquid due to the siphon effect is the root cause of these oscillations, which can exhibit a phase shift among different groups of U-tubes. These oscillations propagate throughout the loop and are associated with the presence of U-tubes. Consequently, PWRs equipped with U-tube SGs are expected to experience siphon condensation oscillations [44]. Experimental findings from the Advanced Plant Experiment-Combustion Engineering test facility indicate that during a SB-LOCA transient, the long tubes in SGs exhibit earlier drainage than the short tubes. Nevertheless, the current practice in several safety analysis codes is to aggregate the SG U-tube bundle into a singular tube, leading to increased prediction uncertainty [45],[44].

4.4.3. Critical/Choked Flow

Safety assessments of water-cooled nuclear reactors are significantly influenced by critical flow, which governs inventory loss in the system. This phenomenon occurs in pipes, valves, and RCS breaks. The discharge flow is a crucial factor in determining the depressurization rate of the system, the heat transfer within the core, and the pressurization behavior of the containment. The critical flow rate is widely acknowledged to be contingent on the stagnation condition of the fluid, the entrance geometry, and the length-to-diameter ratio of the test section. As shown in Fig. 15, when the pressure in the downstream environment (P_D) is gradually reduced, the velocity increases until it reaches a certain threshold, beyond which further reduction in downstream pressure has no impact on the upstream behavior. These same principles apply to the pressure profile as well.

The underlying physical explanation for this phenomenon is that when the pressure falls below P_D, the speed of sound becomes dominant in the exit section. As a result, no information or disturbances can be transmitted upstream beyond this point. This condition is commonly referred to as “choked flow,” indicating that the flow is restricted and unable to propagate upstream. Generally, the occurrence of critical flow can be attributed to the substantial expansion of the gaseous phase. This phenomenon can be understood by considering energy-conservation principles, specifically the conversion of potential energy into kinetic energy [38]. The speed of sound can be defined from Eq. (1).

(1)

The maximum flow rate value at the break is constrained by the critical flow rate. As a result, there is a significant need for reliable and (preferably) conservative models. These models should accurately account for the limitations imposed by the critical flow rate, ensuring that the estimated flow rates remain within safe, reliable limits. Use of such models becomes crucial to prevent potential system failures or inaccuracies that could arise from overestimating the flow rates. The transition from critical to subcritical flow requires careful prediction, particularly when shifting from a flow rate calculated using critical flow models to one predicted by simple momentum equations [38],[46].

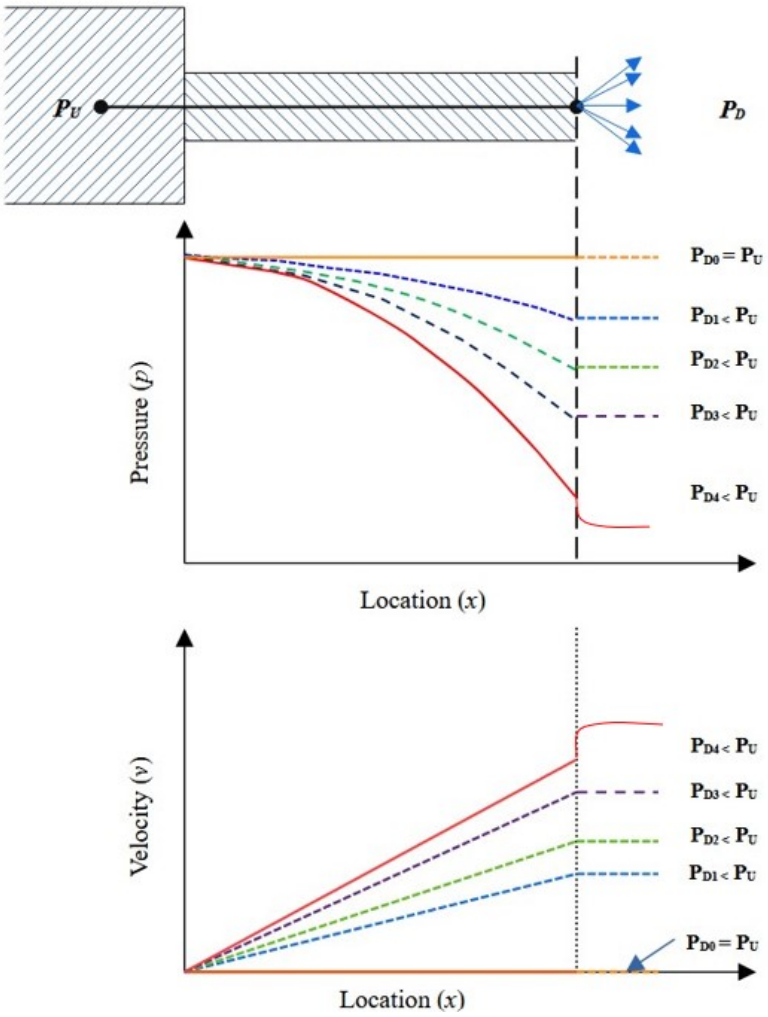

Fig. 15. Critical flow phenomena.

4.4.4. Counter-Current Flow Limitation

As mentioned earlier, in reflux condensation, the occurrence of CCFL or flooding is related to steam velocity, which can trigger a disruptive disturbance at the steam-liquid interface. The onset of CCFL is marked by significant waves on the interface, turbulent flow, and a heightened pressure drop in the gas phase. This phenomenon plays a crucial role in determining the maximum velocity of one phase relative to the other, such that neither can undergo any further velocity increase without altering the flow regime. CCFL can arise in various flow structures that feature changes in flow direction or area, including the upper-core tie plate, downcomer, hot-legs (see Fig. 16), SGs, and pressurizer surge line. CCFL is of critical concern in PWR safety analyses and is an essential element when investigating the horizontal and inclined portions of hot-legs connected to SGs, as well as the uphill side of the SG U-tubes and pressurizer surge line during SB-LOCA transients [42],[47],[48].

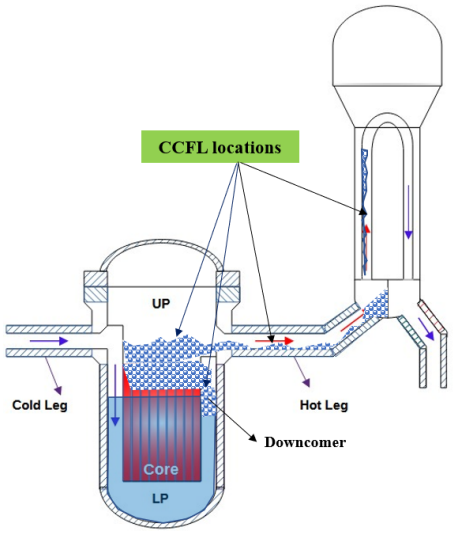

Fig. 16. CCFL locations in PWRs with U-tube SGs.

4.4.5. Entrainment

In contrast to large-break LOCA scenarios, depressurization rates during SB-LOCA transients tend to be slower, which leads to the separation of liquid and steam phases within the RCS. This separation results in various phase-separation effects that influence the thermal-hydraulic characteristics of the system. Liquid entrainment—notably branch entrainment (from the hot-legs to the ADS-4) and pool entrainment (from the upper plenum to the hot-legs)—has been a focal point of concern during the safety analysis of the AP1000. When the ADS-4 valves open, steam is vented directly into the containment. Branch entrainment can occur if steam velocity is sufficiently high. Liquid entrainment in the hot-legs can significantly affect the flow quality and critical flow rate out of the ADS-4, ultimately determining the depressurization rate and system inventory. Given that the working fluid is an air-water mixture, the ongoing phase changes between steam and water necessitate careful consideration when dealing with the branch entrainment rate [38],[41],[42].

4.4.6. Pressurized Thermal Shock

Pressurized thermal shock (PTS) is a critical phenomenon that raises concerns in the field of nuclear engineering due to its potential impact on the structural integrity of PWR vessels. PTS can be influenced by the rapid depressurization of the primary system, as well as overfeed caused by the introduction of highly borated water by the high-pressure injection system. While these actions can reduce mass transfer from the primary to the secondary system and decrease the amount of radioactivity release from the primary side, they also create a heightened risk for the development of PTS [38],[49].

4.4.7. Boron Dilution/Risks

In nuclear systems, flow reversal at the ruptured SG—specifically from the secondary to the primary system—can have two consequences. It can halt the release of radioactivity into the SG while allowing the entry of de-borated liquid into the primary coolant. Consequently, emergency operating procedures have been designed to maintain close pressure alignment between the primary side and SG—with an appropriate margin—to prevent the occurrence of such phenomena [38]. Furthermore, following cold-leg LOCA boron concentration can be built up in the core. Once the water recirculation stops in the SG and PRHRS heat exchanger, boron begins to build up in the core. The borated water sources are established through the initiation of the CMT and the chemical and volume control system.

4.4.8. Hydrogen Risk

In the event of a SB-LOCA, it is imperative to carefully assess the hydrogen-related risks as a critical factor. Previous analyses have been conducted to study the hydrogen risks in NPPs. The potential for hydrogen combustion has been performed in the Advanced Power Reactor 1400 MWe (APR1400) containment during a severe accident triggered by a SB-LOCA using multi-dimensional hydrogen analysis system (MHAS) [50]. The results demonstrated that the calculated peak pressure resulting from flame acceleration is approximately 0.555 MPa, which is below the fracture pressure of the APR1400 containment. This suggests that the structural integrity of the APR1400 containment can be preserved even in the event of hydrogen combustion during a severe accident initiated by SB-LOCA. Another study analyzed the hydrogen risks in marine NPP under LOCA event using 3-D CFD GASFLOW code [51],[52],[53]. It was observed that in the absence of hydrogen mitigation measures, it is probable that hydrogen explosion and flame acceleration could occur during LOCA. While the pressure and temperature in the cabin remain below their design limits, the occurrence of a hydrogen explosion poses a significant risk of damaging both equipment and endangering the structural integrity of the cabin. The release of radionuclides was analyzed during severe accident following SB-LOCA using MELCOR code [54], [55]. The analysis of hydrogen source term release revealed that the maximum hydrogen release was 248.567 kg due to the core support plate failure. However, it is noteworthy that the released hydrogen volume constituted less than 4% of the air volume, indicating the absence of any potential for hydrogen explosion accidents [55]. Accident like steam generator tube rupture in water-cooled SMRs could also lead to a direct path for radionuclides to be released to the atmosphere via the safety and relief valves, making assessments of radionuclide discharge from operating nuclear power plants (NPPs) into the environment crucial for ensuring safety [56], [57]. Studies showed that multicomponent steam-gas mixture—hydrogen, air, and steam mixture in reactor containment during a steam release and fuel failure accident scenarios—parametric and CFD results showed consistent for hydrogen (substituted by helium) percentage ranged of 0%–20% for SMR containment passive safety analysis [58], [59].

The aforementioned phenomena are associated with SB-LOCA scenario in different components and location in the AP1000 reactor. The previous phenomena are the most common during SB-LOCA transient. Thus, understanding the behavior of those phenomena will help in designing and licensing of the recent and new generation reactors as well as designing the IET and SET facilities. It is essential to emphasize that the existing models employed for critical flow, CCFL, and entrainment are derived from experimental data collected under conditions that significantly diverge from those encountered during reactor operation. Hence, it is imperative to conduct investigations under high-pressure and high-temperature conditions. Additionally, the development of new models that accurately capture intricate mechanisms is indispensable for enhancing the robustness of system safety analysis codes.

5. Conclusion

PSSs play a pivotal role in advanced reactor system design and development, ensuring both safety and reliability. PSS performance can be improved by incorporating new materials and technologies, such as advanced heat exchangers and PCCSs. This study reviewed the PSS for a reference PWR considered representative of the processes that would occur in the context of SMRs. The accident progression was presented in tandem with a comprehensive review of the details pertaining to the physics phenomena. This review and its related findings support the following goals:

- Describing reactor systems that feature similar design criteria (e.g., water-cooled passive SMRs)
- Designing and verifying the PSS of the new reactor system by using computer code models
- Developing integral effect tests and separate effect test facilities to obtain test data for supporting computer code model development and assessment
- Using and selecting appropriate instruments and sensors to measure important physics parameters
- Preparing an adequate test matrix to perform the required testing, considering accident events and phases

- Validating computer codes (i.e., system codes) and simulation models through uncertainty qualifications
- Standardizing accident management, safety protocols, and emergency responses, with adequate training.

These studies widen the scope of evaluation for new reactor-design approaches by including, for example, different coolants or fuels that afford greater damage resistance during LOCAs. Evaluating and comparing these design options requires a thorough understanding of the physical phenomena involved in LOCAs and the performance of PSSs.

This study and its findings can be useful in evaluating human and operational factors pertaining to nuclear reactor system accident management. Effective training programs, clear communication protocols, and a strong safety culture can help prevent accidents and ensure that PSSs are correctly implemented. Emergency response plans and procedures should also be regularly tested and updated to ensure their effectiveness in the event of accidents.

Understanding the accident-event progression and associated physical phenomena of LOCAs is crucial for designing and evaluating water-cooled SMR PSSs. This requires using thermal-hydraulics models and supportive test datasets to simulate reactor behavior and evaluate PSS performance. Additionally, improving the safety and reliability of NPPs requires considering human/organizational factors and continually exploring new design options and technologies.

Acknowledgments

This research was funded by United State (U.S.) Department of Energy (DOE) Advanced Reactor Demonstration Project (ARDP) program office grant number ARDP-20-23819. Funding Opportunity Number DE-FOA-0002271, Risk Reduction Pathway. The authors would like to thank the U.S. DOE National Reactor Innovation Center (NRIC) ARDP program office and Irradiation Experiment and Thermal Hydraulics Analysis Department at Idaho National Laboratory (INL) for the encouragement and support.

Disclaimer

References

1. Westinghouse. (1994). “AP600 design change description report,” Proprietary Class 2C Report. Westinghouse Electric Company, LLC, Pittsburgh, PA, USA.
2. Sun, H., Y. Zhang, W. Tian, S. Qiu, and G. Su. (2020). “Performance analysis of automatic depressurization system in advanced PWR during a typical SBLOCA transient using MIDAC.” *Nucl. Eng. Technol*., 52(5), 937–946. https://doi.org/10.1016/j.net.2019.10.011.
3. Li, Y., Z. Ye, J. Zhang, and H. Chang. (2020). “Core makeup tank behavior investigation during ACME integral effect tests.” *Nucl. Eng. Des.*, 364, 110701. https://doi.org/10.1016/j.nucengdes.2020.110701.
4. Choi, K., S. Cho, K. Kang, H. Park, and Y. Kim. (2014). “Comparison of integral thermal-hydraulic behaviors of a DVI line break SBLOCA with an equivalent cold leg break.” *Nucl. Eng. Des.*, 273,

421–434. https://doi.org/10.1016/j.nucengdes.2014.02.033.

5. Jeong, J. J., K. S. Ha, B. D. Chung, and W. Lee. (1999). "Development of a multi-dimensional thermal-hydraulic system code, MARS 1.3.1." *Ann. Nucl. Energy*, 26(18), 1611–1642. https://doi.org/10.1016/s0306-4549(99)00039-0.
6. Qiu, Z., H. Yu, Q. Xiong, X. Cao, and L. Tong. (2023). "Uncertainty and sensitivity analysis of the DVI line break loss of coolant accident for small modular reactor. *Prog. Nucl. Energy*, 157, 104575. https://doi.org/10.1016/j.pnucene.2023.104575.
7. Kim, Y., H. Bae, B. Jeon, Y. Bang, S. Yi, and H. Park. (2018). "Investigation of thermal hydraulic behavior of SBLOCA tests in SMART-ITL facility." *Ann. Nucl. Energy*, 113, 25–36. https://doi.org/10.1016/j.anucene.2017.11.013.
8. Wang, H., C. Xu, K. Cao, H. Chang, and P. Chen. (2017). "ADS-IRWST transient evaluation model for AP1000 SBLOCA analysis," *Ann. Nucl. Energy*, 100(2), 169–177. https://doi.org/10.1016/j.anucene.2016.08.027.
9. Schulz, T. L. (2006). "Westinghouse AP1000 advanced passive plant." *Nucl. Eng. Des.,* 236(14–16), 1547–1557. https://doi.org/10.1016/j.nucengdes.2006.03.049.
10. Zeliang, C., Y. Mi, A. Tokuhiro, L. Lu, and A. Rezvoi. (2020). "Integral PWR-type small modular reactor developmental status, design characteristics and passive features: A review." *Energies*, 13(11), 2898. https://doi.org/10.3390/en13112898.
11. Ahn, K. I., K. H. Lee, S. W. Lee, G. Choi, and S. W. Hwang. (2021). "Estimation of fission product source terms for the SGTR accident of a reference PWR plant using MELCOR and MAAP5." *Nucl. Eng. Des.*, 371, 110967. https://doi.org/10.1016/j.nucengdes.2020.110967.
12. Bhowmik, P. K., S. J. Ormiston, J. P. Schlegel, and D. Chowdhury. (2023). "State-of-the-art and review of condensation heat transfer for small modular reactor passive safety: Computational studies." *Nuclear Engineering and Design*, 410, 112366. https://doi.org/10.1016/j.nucengdes.2023.112366.
13. Bhowmik, P. K., J. P. Schlegel, and S. Revankar. (2022). "State-of-the-art and review of condensation heat transfer for small modular reactor passive safety: Experimental studies." *Int. J. Heat Mass Transf.*, 192, 122936. https://doi.org/10.1016/j.ijheatmasstransfer.2022.122936.
14. Zhang, J., and C. Schneidesch. (2023). "Application of the BEPU safety analysis method to quantify margins in nuclear power plants." *Nucl. Eng. Des.*, 406, 112233. https://doi.org/10.1016/j.nucengdes.2023.112233.
15. Auvinen, A., J. K. Jokiniemi, A. Lähde, T. Routamo, P. Lundström, H. Tuomisto, J. Dienstbier, S. Güntay, D. Suckow, A. Dehbi, M. Slootman, L. Herranz, V. Peyres, and J. Polo. (2005). "Steam generator tube rupture (SGTR) scenarios." *Nucl. Eng. Des.,* 235(2–4), 457-472. https://doi.org/10.1016/j.nucengdes.2004.08.060.
16. Bhowmik, P. K., C. E. E. Perez, J. D. Fishler, S. A. B. Prieto, I. D. Reichow, J. T. Johnson, P. Sabharwall, and J. E. O'Brien. (2023). "Integral and separate effects test facilities to support water cooled small modular reactors: A review." *Prog. Nucl. Energy*, 160, 104697. https://doi.org/10.1016/j.pnucene.2023.104697.
17. Kamalpour, S., & Khalafi, H. (2021). SMART reactor core design optimization based on FCM fuel. *Nuclear Engineering and Design*, *372*, 110970. https://doi.org/10.1016/j.nucengdes.2020.110970.
18. AP300™ Small Modular Reactor. https://www.westinghousenuclear.com/energy-systems/ap300-smr.
19. Hussein, E. M. (2020). Emerging small modular nuclear power reactors: A critical review. *Physics Open*, 5, 100038. https://doi.org/10.1016/j.physo.2020.100038.
20. Westinghouse. (2023). "Nuclear safety – Unequaled design." Westinghouse Electric Company, LLC, Pittsburgh, PA, USA. Available at: https://www.westinghousenuclear.com/energy-systems/ap1000-pwr/safety (accessed 13 November 2023).

21. Corletti, M. M. (2000). “AP1000 Plant Description and Analysis Report.” Technical Report, WCAP-15612, Westinghouse Electric Company, LLC, Pittsburgh, PA, USA. Available at: https://www.nrc.gov/docs/ml0037/ML003779406.pdf (accessed 13 November 2023).
22. Lioce, D., M. Asztalos, A. Alemberti, L. Barucca, M. Frogheri, and G. Saiu. (2012). “AP1000 passive core cooling system preoperational tests procedure definition and simulation by means of Relap5 Mod. 3.3 computer code.” *Nucl. Eng. Des*., 250, 538–547. https://doi.org/10.1016/j.nucengdes.2012.05.028.
23. Westinghouse. (2011). “Accident Analyses,” in *AP1000 Design Control Document*. Technical Report, Revision 19, Chapter 15, ML11171-A367, Westinghouse Electric Company, LLC, Pittsburgh, PA, USA. Available at: https://www.nrc.gov/docs/ML1117/ML11171A367.pdf (accessed 13 November 2023).
24. Yang, J., W. W. Wang, S. Z. Qiu, W. X. Tian, G. H. Su, and Y. W. Wu. (2012). “Simulation and analysis on 10-in. cold leg small break LOCA for AP1000.” *Ann. Nucl. Energy*, 46, 81–89. https://doi.org/10.1016/j.anucene.2012.03.007.
25. Elshahat, A. E., T. Abram, J. K. Hohorst, and C. M. Allison. (2014). “Simulation of the Westinghouse AP1000 response to SBLOCA using RELAP/SCDAPSIM.” *Int. J. Nucl. Energy*, 2014, 410715. https://doi.org/10.1155/2014/410715.
26. Wright, R. F. (2007). “Simulated AP1000 response to design basis small-break LOCA events in APEX-1000 test facility.” *Nucl. Eng. Technol.*, 39(4), 287–298. https://doi.org/10.5516/NET.2007.39.4.287.
27. Westinghouse. (2004). “AP1000 Design Control Document.” Technical Report, Revision 18, Westinghouse Electric Company, LLC, Pittsburgh, PA, USA.
28. Boyack, B. E., and J. F. Lime. (1995). “Intermediate-break LOCA analyses for the AP600 design.” LA-UR-95-1785, Los Alamos National Laboratory, Los Alamos, NM, USA. https://doi.org/10.2172/105674.
29. Montero-Mayorga, J., C. Queral, and J. Gonzalez-Cadelo. (2015). “AP1000® SBLOCA simulations with TRACE code.” *Ann. Nucl. Energy*, 75, 87–100. https://doi.org/10.1016/j.anucene.2014.07.045.
30. Westinghouse. (2008). “AP1000 Design Control Document.” Technical Report, Revision 17, Westinghouse Electric Company, LLC, Pittsburgh, PA, USA. Available at: https://www.nrc.gov/docs/ML0832/ML083230868.html. (accessed 13 November 2023).
31. Westinghouse. (2003). “AP1000 Probabilistic Risk Assessment Report.” Technical Report, Rev. 1, Westinghouse Electric Company, LLC, Pittsburgh, PA, USA.
32. Meyer, P. E. (1985). “NOTRUMP—A Nodal Transient Small-Break and General Network Code.” WCAP-10079-P-A (Proprietary) and WCAP-10080-A (Nonproprietary). U.S. Nuclear Regulatory Commission, Washington, D.C., USA.
33. 10 CFR 50.46, “Acceptance Criteria for Emergency Core-Cooling Systems for Light Water-Cooled Nuclear Power Reactors,” and Appendix K to 10 CFR 50, “ECCS Evaluation Models.” U.S. Nuclear Regulatory Commission, Washington, D.C., USA. Available at: https://www.nrc.gov/reading-rm/doc-collections/cfr/part050/part050-0046.html (accessed 13 November 2023).
34. Wilson, G. E., C. D. Fletcher, C. B. Davis, J. D. Burtt, and T. J. Boucher. (1997). “Phenomena Identification and Ranking Tables for Westinghouse AP600 Small Break Loss-Of-Coolant Accident, Main Steam Line Break, and Steam Generator Tube Rupture Scenarios.” NUREG/CR-6541-Rev.2; INEL-94/0061-Rev.2, U.S. Nuclear Regulatory Commission, Washington, D.C., USA. https://doi.org/10.2172/501518.
35. Brown, W., and R. Ofstun. (2001). “PIRT/scaling assessment for AP1000.” *International Conference on Nuclear Engineering*, 8–12 April 2001, Nice, Acropolis, France. Available at: https://www.osti.gov/etdeweb/biblio/20232080 (accessed 13 November 2023).
36. Yuquan, L., H. Botao, Z. Jia, and W. Nan. (2017). “Comparative experiments to assess the effects of accumulator nitrogen injection on passive core cooling during small break LOCA.” *Nucl. Eng.*

Technol., 49(1), 54–70. https://doi.org/10.1016/j.net.2016.06.014.

37. D'Auria, F., and M. Frogheri. (2002). "Use of a natural circulation map for assessing PWR performance." *Nucl. Eng. Des.*, 215(1–2), 111–126. https://doi.org/10.1016/S0029-5493(02)00045-6.
38. D'Auria, F. (2017). *Thermal-Hydraulics of Water-Cooled Nuclear Reactors*. Woodhead Publishing, Sawston, United Kingdom. https://doi.org/10.1016/B978-0-08-100662-7.09994-2.
39. Wang, W. W., G. H. Su, S. Z. Qiu, and W. X. Tian. (2011). "Thermal hydraulic phenomena related to small break LOCAs in AP1000." *Prog. Nucl. Energy*, 53(4), 407–419. https://doi.org/10.1016/j.pnucene.2011.02.007.
40. D'Auria, F. (2009). "Natural circulation situations relevant to nuclear power plants." *Joint ICTP-IAEA Course on Natural Circulation Phenomena and Passive Safety Systems in Advanced Water-Cooled Reactors (SMR 2349)*, 3–7 December 2012, Trieste, Italy.
41. De Santi, G., L. Piplies, and J. Sanders. (1986). "Mass flow instabilities in LOBI steam generators U-tubes under natural circulation conditions." in Wakabayashi, J., and H. Nariai (eds.), *Second International Meeting on Nuclear Power Plant Thermal-Hydraulics and Operations*, 15–17 April 1986, Tokyo, Japan. pp. 2/158–2/165.
42. Lee, N. (1987). "Limiting countercurrent flow phenomenon in small break LOCA transients." *Nucl. Eng. Des.*, 102(2), 211–216. https://doi.org/10.1016/0029-5493(87)90254-8.
43. Tasaka, K., Y. Kukita, Y. Koizumia, M. Osakabe, and H. Nakamura. (1988). "The results of 5% small-break LOCA tests and natural circulation tests at the ROSA-IV LSTF." *Nucl. Eng. Des.*, 108(1–2), 37–44. https://doi.org/10.1016/0029-5493(88)90054-4.
44. D'Auria, F., and G. M. Galassi. (1990). "Flowrate and density oscillations during two-phase natural circulation in PWR typical conditions." *Nucl. Eng. Des.*, 122(1–3), 209–218. https://doi.org/10.1016/0029-5493(90)90207-E.
45. Reyes, J. N., Jr. (2004). "Flow stagnation and thermal stratification in single and two-phase natural circulation loops." in *Natural Circulation in Water-Cooled Nuclear Power Plants*, ANNEX 15, IAEA-TECDOC-1474, International Atomic Energy Agency, Vienna, Austria. pp. 433–460. Available at: https://inis.iaea.org/collection/NCLCollectionStore/_Public/37/032/37032143.pdf?r=1 (accessed 13 November 2023).
46. Minato, A., R. Kawabe, H. Yamanouchi, and H. Kato. (1979). "SENHOR-IV: A computer code for small pipe-break analysis of pressure-tube type reactors." *Nucl. Eng. Des.*, 53(3), 377–385. https://doi.org/10.1016/0029-5493(79)90064-5.
47. Wongwises, S. (1996). "Two-phase countercurrent flow in a model of a pressurized water reactor hot-leg." *Nucl. Eng. Des.*, 166(2), 121–133. https://doi.org/10.1016/0029-5493(96)01272-1.
48. Solmos, M., K. J. Hogan, and K. Vierow. (2009). "Flooding Experiments and Modeling for Improved Reactor Safety." *U.S.-Japan Two-Phase Flow Seminar*, 14–18 September 2008, Santa Monica, CA, USA. Available at: https://www.osti.gov/servlets/purl/936720 (accessed 13 November 2023).
49. Jhung, M. J., S. H. Kim, Y. H. Choi, Y. S. Chang, X. Xu, J. M. Kim, J. W. Kim, and C. Jang. (2010). "Probabilistic fracture mechanics round robin analysis of reactor pressure vessels during pressurized thermal shock." *J. Nucl. Sci. Technol.*, 47(12), 1131–1139. https://doi.org/10.1080/18811248.2010.9720980.
50. Kang, H.-S., J. Kim, and S.-W. Hong. (2022). "Numerical analysis for hydrogen flame acceleration during a severe accident initiated by SBLOCA in the APR1400 containment." *Hydrogen*, 3(1), 28–42. https://doi.org/10.3390/hydrogen3010002.
51. Zhao, H., X. Luo, R. Zhang, X. Lyu, H. Yin, and Z. Kang. (2021). "Analysis on hydrogen risk under LOCA in marine nuclear reactor." *Exp. Comput. Multiph. Flow*, 4(1), 39–44. https://doi.org/10.1007/s42757-020-0077-2.
52. Huang, X.-G., and Y.-H. Yang. (2011). "Analysis of characters and efficiency for ignitor in hydrogen mitigation system." *Yuanzineng Kexue Jishu/At. Energy Sci. Technol*., 45(6), 716–721.

Available at: https://www.researchgate.net/publication/286381352 (accessed 13 November 2023).

53. Meng, X., X. Lu, B. Wang, S. Liu, Y. Yu, and Z. Guo. (2020). "The measure on mitigating hydrogen risk during LOCA accident in nuclear power plant." *Ann. Nucl. Energy*, 136, 107032. https://doi.org/10.1016/j.anucene.2019.107032.
54. Fang, Z., Z. Shuliang, L. Zejun, X. Tao, X. Shoulong, H. Yan, and F. Jinjun. (2021). "Study on release and migration of radionuclides under the small break loss of coolant accident in a marine reactor." *Sci. Technol. Nucl. Install.*, 2021, 1–12. https://doi.org/10.1155/2021/6635950.
55. Bhowmik, P. K., & Sabharwall, P. (2023). Sizing and Selection of Pressure Relief Valves for High-Pressure Thermal–Hydraulic Systems. Processes, 12(1), 21. https://doi.org/10.3390/pr12010021.
56. Abdellatif, H. H., Bhowmik, P. K., Arcilesi, D., & Sabharwall, P. (2024). Accident event progression, gaps, and key performance indicators for steam generator tube rupture events in water-cooled SMRs: A review. Progress in Nuclear Energy, 168, 105021. https://doi.org/10.1016/j.pnucene.2023.105021.
57. Bhowmik, P.K., J. P., Schlegel, V., Kalra, S. Alam, S. Hong, S. Usman. (2022). CFD validation of condensation heat transfer in scaled-down small modular reactor applications, Part 1: Pure steam. Exp. Comput. Multiph. Flow, 4(4), 409-423 (2022). https://doi.org/10.1007/s42757-021-0115-5.
58. Bhowmik, P.K., J. P., Schlegel, V., Kalra, S. Alam, S. Hong, S. Usman. (2022) CFD validation of condensation heat transfer in scaled-down small modular reactor applications, Part 2: Steam and non-condensable gas. Exp. Comput. Multiph. Flow 4, 424–434 (2022). https://doi.org/10.1007/s42757-021-0113-7.
59. Bhowmik, P.K., Schlegel, J.P. (2023). Multicomponent gas mixture parametric CFD study of condensation heat transfer in small modular reactor system safety. Exp. Comput. Multiph. Flow 5, 15–28. https://doi.org/10.1007/s42757-022-0136-8.